Vygotsky: Jurnal Pendidikan Matematika dan Matematika
8 (1) February 2026, pp. 51 - 64
E-ISSN: 2656-5846 P-ISSN: 2656-2286
Journal Page is available to
https://jurnalpendidikan.unisla.ac.id/index.php/VoJ

Estimation of Dengue Fever Transmission Model in West Java Using the Ensemble Kalman Filter Method

Addinda Nur Ameliyah[1*], Didik Khusnul Arif[1]

[1] Department of Mathematics, Institut Teknologi Sepuluh Nopember, Indonesia

**Email Correspondence:* addinda20@gmail.com

ARTICLE INFO

Article History

Received	:	1 Feb 2026
Revised	:	16 Feb 2026
Accepted	:	26 Feb 2026
Available Online	:	28 Feb 2026

Keywords:
Dengue Fever Transmission
Ensemble Kalman Filter
Unscented Kalman Filter
Nonlinear Dynamics
SEIRSI Model

Please cite this article APA style as:
Ameliyah, A. N. & Arif, D. K. (2026). Estimation of Dengue Fever Transmission Model in West Java Using the Ensemble Kalman Filter Method. *Vygotsky: Jurnal Pendidikan Matematika dan Matematika*, 8(1), pp. 51-64.

ABSTRACT

Dengue Fever Transmission is a serious, potentially fatal infectious if unmanaged disease. It caused by the dengue virus, transmitted by Aedes aegypti and Aedes albopictus mosquitoes. In West Java, cases remain high and fluctuate significantly, requiring precise mathematical modeling to describe transmission dynamics. This is the first study applying Ensemble Kalman Filter (EnKF) in West Java to estimate the SEIR-SI model, compared to Unscented Kalman Filter (UKF), using dengue fever transmission case data from 2010–2023. Performance was assessed via Mean Absolute Percentage Error (MAPE) for the infected human population (I_h), showing EnKF's superior accuracy (2.4%) over UKF (7.8%). EnKF effectively estimates hard-to-measure epidemiological variables and this study can support government prediction-based dengue fever transmission control policies.

Vygotsky: Jurnal Pendidikan Matematika dan Matematika with CC BY NC SA license
Copyright © 2026, The Author (s)

1. Introduction

Dengue fever transmission is an infectious disease caused by the dengue virus and transmitted through the bites of *Aedes mosquitoes*, primarily *Aedes aegypti* and *Aedes albopictus* (Messina et al., 2020) . The dengue virus belongs to the genus *Flavivirus* of the *Flaviviridae* family and consists of four distinct serotypes, namely DEN-1, DEN-2, DEN-3, and DEN-4 (World Health Organization, 2024)(Papa et al., 2024). Dengue infection is characterized by an incubation period of approximately 4–10 days, followed by clinical manifestations such as persistent high fever, skin rash,

E-ISSN: 2656-5846
P-ISSN: 2656-2286

gastrointestinal symptoms, and a significant decrease in platelet count (Narinder, Ajeet, and Amar, 2022)(Namirimu and Kim, 2024). The critical phase typically occurs between the third and seventh day of illness and may lead to serious complications, including plasma leakage, severe bleeding, and dengue shock syndrome, which can be fatal if not properly managed (Kularatne et al., 2025).

Globally, dengue fever transmission remains a major public health concern, particularly in tropical and subtropical regions where more than half of the world's population is at risk of dengue fever transmission (World Health Organization, 2024)(Zhang et al., 2025). The life cycle and population dynamics of *Aedes aegypti* as the primary vector are strongly influenced by climatic factors such as temperature, humidity, and rainfall patterns (Liu et al., 2023). In the context of global climate change, extreme climate phenomena such as El Niño further exacerbate environmental conditions by increasing average temperatures and altering rainfall variability (Bolan et al., 2024). These conditions accelerate mosquito reproduction cycles and increase biting frequency, thereby elevating the risk of dengue fever transmission (Nasirian, 2024)(Awaludin, Prayitno, and Haq, 2023).

In Indonesia, dengue fever transmission has become an endemic disease with a noticeable increase in reported cases over recent years. Official records indicate that dengue cases rose from 73,518 cases with 705 deaths in 2021 to 143,000 cases with 1,236 deaths in 2022. By the 43rd week of 2024, the number of reported cases surged to 210,644, accompanied by 1,239 fatalities. The high incidence of dengue is closely associated with population density, particularly on Java Island. Provinces such as West Java, East Java, and Central Java consistently report the highest number of cases, with West Java recording the largest burden due to rapid urbanization, dense settlements, and limitations in vector control infrastructure (Kementerian Kesehatan Republik Indonesia, 2024).

The persistent increase in dengue cases highlights the need for a systematic understanding of the disease transmission dynamics (Zeng et al., 2023). Such understanding requires accurate estimation of state variables within a dynamic disease transmission model. Mathematical modeling has been widely employed to represent the spread of infectious diseases, especially for systems in which several components cannot be directly observed. Estimation techniques play a crucial role in inferring unobservable variables based on available observational data, making them particularly important for complex nonlinear epidemiological systems. Several studies have explored estimation approaches in infectious disease modeling. (Safitria, Arif, and Fatmawati, 2023) applied the Ensemble Kalman Filter (EnKF) to a nonlinear continuous malaria transmission model in Indonesia using cumulative case data from 2010–2022, incorporating forward finite difference discretization and linearization prior to assimilation; the results yielded a low RMSE of 0.005, indicating strong alignment with observational data, though the linearization step may constrain accuracy under extreme nonlinearity.

Other works have extended EnKF to dengue. For instance, (Cohnstaedt and Scoglio, 2021) proposed an SEIR-SEI-EnKF framework for dengue outbreak estimation and forecasting, showing improved performance over simpler models like SIR-EnKF or SEIR-EnKF in both simulations and real-world data. (Papageorgiou and Tsaklidis, 2022) developed a hybrid SEIHCRDV-UKF model for COVID-19 prediction, effectively estimating time-dependent parameters and unobserved states in complex epidemiological systems.

E-ISSN: 2656-5846
P-ISSN: 2656-2286

Although these approaches have proven effective for outbreak prediction in endemic regions of China, similar applications to the dengue SEIR–SI model remain limited, particularly when using regional data from Indonesia such as West Java Province. Prior studies have largely focused on short- to medium-term forecasting rather than precise state variable estimation to directly inform control strategies (e.g., estimating unobserved latent infections, infected vectors, or recovered individuals). Moreover, direct comparisons between EnKF and the Unscented Kalman Filter (UKF) on local dengue datasets have received little attention, despite the methods' differing trade-offs in addressing nonlinearity, data noise, and computational demands across varying state dimensions.

This study bridges these gaps by applying EnKF to a tailored SEIR–SI dengue model in West Java, capitalizing on ensemble flexibility for more accurate state estimation in complex nonlinear systems with local observational data. A comparative analysis with UKF serves as validation to assess the relative effectiveness and precision of both methods in this context. The results of this study are expected to provide a strong quantitative basis for health authorities in establishing more consistent and data-based dengue control and prevention strategies.

2. Method

The methods employed in this study include SEIR–SI modeling for dengue transmission, discretization of the differential equations, and the application of EnKF and UKF for state variable estimation and model performance evaluation.

2.1. SEIRSI Model for Dengue Fever Transmission

Dengue fever transmission can be represented using various host–vector frameworks that describe how infections move between human and mosquito populations. Such formulations typically extend compartment-based models to incorporate biological processes, incubation periods, and vector dynamics, ensuring that the resulting system better reflects real epidemiological behavior. In this study, the dengue fever transmission model employed is an extension of the nonlinear host–vector model proposed by (Wijayanti and Fakhruddin, 2023).

A time-dependent host–vector model for dengue fever transmission was developed by incorporating an SEIR framework for the human population and an SI framework for the mosquito population. In this model, the human population is categorized into susceptible (S_h), exposed (E_h), infected (I_h), and recovered (R_h) groups, while the mosquito population is divided into susceptible (S_v) and infected (I_v) classes.

Time-varying transmission rates for both humans and vectors are applied to account for unobservable factors that influence the transmission dynamics. The transition processes between compartments are illustrated in Figure 1. Based on this formulation, a compartmental diagram was constructed to represent the spread of dengue fever transmission as follows.

https://doi.org/10.30736/voj.v8i1.1325

E-ISSN: 2656-5846
P-ISSN: 2656-2286

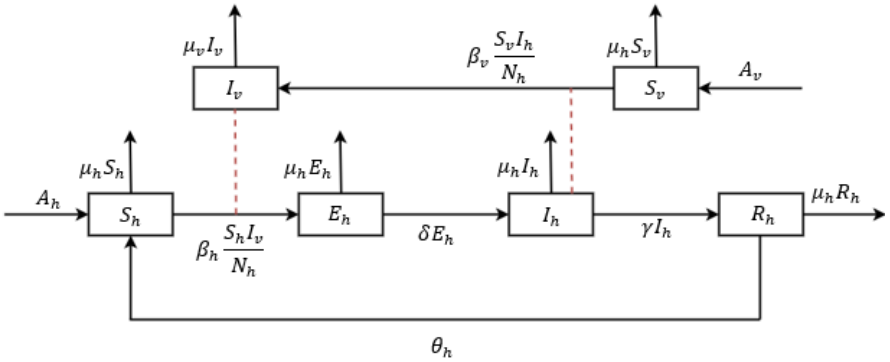

Figure 1. Compartment Diagram of the Dengue Fever Transmission Model

$$\frac{dS_h}{dt} = \Lambda_h - \beta_h \frac{S_h I_v}{N_h} - \mu_h S_h + \theta R_h \quad (1)$$

$$\frac{dE_h}{dt} = \beta_h \frac{S_h I_v}{N_h} - \delta E_h - \mu_h E_h \quad (2)$$

$$\frac{dI_h}{dt} = \delta E_h - \gamma I_h - \mu_h I_h \quad (3)$$

$$\frac{dR_h}{dt} = \gamma I_h - \mu_h R_h - \theta R_h \quad (4)$$

$$\frac{dS_v}{dt} = \Lambda_v - \beta_v \frac{S_v I_h}{N_h} - \mu_v S_v \quad (5)$$

$$\frac{dI_v}{dt} = \beta_v \frac{S_v I_h}{N_h} - \mu_v I_v \quad (6)$$

The parameters used in the system are defined as follows.

S_h : Human population susceptible to dengue transmissio
E_h : Human population exposed to the dengue virus but not yet infectious
I_h : Human population infected and capable of transmitting the virus
R_h : Recovered human population
S_v : *Aedes* mosquito population not yet infected and potentially contract the virus after contact with an infected human
I_v : Mosquito population infected and capable of transmitting the dengue virus throughout its life
N_h : Total human population
N_v : Total mosquito population
Λ_h : Human birth/growth rate
Λ_v : Mosquito birth/growth rate
μ_h : Natural human mortality (death) rate
μ_v : Natural mosquito mortality (death) rate
β_h : Transmission rate of the virus from infected mosquitoes to susceptible Humans
β_v : Transmission rate of the virus from infected humans to susceptible Mosquitoes
δ : Transition rate from exposed humans (E_h) to infected (I_h)
γ : Transition rate from infected humans (I_h) to recovered (R_h)
θ : Rate of waning immunity in humans

E-ISSN: 2656-5846
P-ISSN: 2656-2286

2.2. Model Discretization

The dynamic model equations describing the spread of Dengue Fever are formulated as continuous differential equations. In order to perform variabel estimation, the differential equation model must be expressed in a discrete form; therefore, a discretization process is required (Villela, 2020). Model discretization can be carried out using several numerical methods, one of which is the forward finite difference method.

If $S = S(x)$ is expanded using a Taylor series, the following expressions are obtained,

$$S(x+h) = S(x) + h\frac{d}{dx}S(x) + \frac{h^2}{2!}\frac{d^2}{dx^2}S(x) + \cdots$$
$$S(x-h) = S(x) - h\frac{d}{dx}S(x) + \frac{h^2}{2!}\frac{d^2}{dx^2}S(x) + \cdots$$

In this study, the forward finite difference method is employed. The numerical scheme of the forward finite difference method is given by,

$$S(x+h) - S(x) = h\frac{d}{dx}S(x) + O(h^2)$$

Thus, the first-order derivative can be approximated as,

$$\frac{dS}{dx} \approx \frac{S(x+h) - S(x)}{h} \tag{7}$$

Equation (7) represents the forward finite difference approximation. Using finite difference notation with $u(x = kh)$, where $h = \Delta x$ and $k = 1,2,3, \ldots, n$, Equation (7) can be rewritten as (Listosari, 2018),

$$\frac{dS}{dx} = \frac{S^{k+1} - Sk}{\Delta x} \tag{8}$$

2.3. Ensemble Kalman Filter (EnKF)

The Ensemble Kalman Filter (EnKF) is a modified estimation method derived from the Kalman Filter algorithm that can be applied to both linear and nonlinear system models (Carrassi and Bocquet, 2018). The EnKF method was introduced by Evensen in 1994 (Tong, Gu, and Cheng 2024). The estimation process in the EnKF begins by generating a set of $N_e$ensembles with zero mean and constant covariance. These ensembles are generated randomly and are assumed to follow a normal distribution. Based on empirical studies, an adequate number of ensemble members typically ranges from 100 to 500. In the EnKF, error propagation does not require linearization of the model as in the Extended Kalman Filter (EKF). Instead, it is performed directly by independently integrating each ensemble member forward using the nonlinear model operator.

This approach makes the EnKF particularly well-suited for strongly nonlinear systems, as the error statistics are evolved using a Monte Carlo method through the ensemble members (Brajard et al., 2021). In general, the EnKF algorithm consists of two main stages, namely the prediction stage and the correction

E-ISSN: 2656-5846
P-ISSN: 2656-2286

(update) stage (Roger, 2020). In the EnKF framework, the ensemble mean is computed prior to entering the prediction step. The general form of a nonlinear dynamic system in the EnKF can be expressed as follows,

$$x_{k+1} = f(x_k, u_k) + w_k$$

with a linear measurement $z_k \in R^p$, namely,

$$z_k = H_k x_k + v_k$$
$$x_0 \sim N(\bar{x}_0, P_{x0}); \; w_k \sim N(0, Q_k); \; v_k \sim N(0, R_k)$$

where H_k is a measurement matrix that shows which variables can be measured. The EnKF algorithm is presented in Table 1.

Table 1. The EnKF algorithm

System Model and Measurement Model	
	$x_{k+1} = f(x_k, u_k) + w_k, ; w_k \sim (0, Q_k)$ $z_k = H x_k + v_k, \quad ; v_k \sim (0, R_k)$
Initialization	Generate N ensembles based on the initial estimate $\hat{x}_0$, $x_{0,i} = [x_{0,1}, x_{0,2}, x_{0,3}, \dots, x_{0,N}]$ Determine the initial ensemble mean, $\hat{x}_0 = \frac{1}{N}\sum_{i=1}^{N} x_{0,i}$
Prediction Step	$\hat{x}_{\bar{k},i} = f(\hat{x}_{k-1}, u_{k-1}) + w_{k,i}, w_{k,i} \sim (0, Q_k)$ $\hat{x}_{\bar{k}} = \frac{1}{N}\sum_{i=1}^{N} (\hat{x}_{\bar{k},i})$ Error covariance $P_{\bar{k}} = \frac{1}{N-1}\sum_{i=1}^{N} (\hat{x}_{\bar{k},i} - \hat{x}_{\bar{k}})(\hat{x}_{\bar{k},i} - \hat{x}_{\bar{k}})^T$
Correction (Update) Step	$z_{k,i} = z_k + v_{k,i}, v_{k,i} \sim (0, R_k)$ Kalman gain, $K_k = P_k^- H^T (H P_k^- H^T + R_k)^{-1}$ State update, $\hat{x}_{k,i} = \hat{x}_{k,i}^- + K_k (z_{k,i} - H \hat{x}_{k,i}^-)$ $\hat{x}_k = \frac{1}{N}\sum_{i=1}^{N} \hat{x}_{k,i}$ Error covariance, $P_k = [I - K_k H] P_k^-$

(Roger, 2020)

2.4. Unscented Kalman Filter (UKF)

The Unscented Kalman Filter (UKF) is an extension of the Kalman Filter and is generally used to address nonlinear and more complex system problems. The concept involves generating several sampling points (Sigma Points) around the estimated condition based on their covariance (Singh, Mishra, and Chattopadhyay, 2024). These points are then propagated through a nonlinear mapping to obtain more accurate estimates of the mean and covariance of the

E-ISSN: 2656-5846
P-ISSN: 2656-2286

resulting mapping (Munch, Rogers, and Sugihara, 2022).

Based on its application, the UKF method can be applied to variable estimation, parameter estimation, and dual estimation. The UKF was first introduced by Simon J. Julier and Jeffery K. Uhlmann in their paper entitled "A New Extension of the Kalman Filter to Nonlinear Systems" in 1997 (Jiang, Shi, and Moura, 2025). The UKF consists of two stages, similar to the KF: a prediction stage (time update) and a correction stage (measurement update). The UKF's function is to simplify the probability distribution approach for approximating nonlinear functions. The error estimates and covariances of the UKF are obtained using the Unscented Transformation. Unscented transformation is a method used to calculate the statistical value of a random variable that has undergone a nonlinear transformation (Li et al., 2025). The UKF algorithm is presented in Table 2

Table 2. The UKF algorithm

System Model and Measurement Model	
Initialization	$x_{k+1} = f(x_k, u_k) + w_k$ $z_k = H\,x_k + v_k$ $x_0 \sim N(\bar{x}_{0,} P_{x_0}), w_k \sim N(\bar{x}_{0,} Q_k), v_k \sim N(0, R_k)$ $\chi_{i\|k} = [\hat{\chi}_{i\|k} \quad \hat{\chi}_{i\|k} + \sqrt{(L+\lambda)P_{i\|k}} \quad \hat{\chi}_{i\|k} - \sqrt{(L+\lambda)P_{i\|k}}$
	Sigma point, $\chi_{i\|k} = [\hat{\chi}_{i\|k} \quad \hat{\chi}_{i\|k} + \sqrt{(L+\lambda)P_{i\|k}} \quad \hat{\chi}_{i\|k} - \sqrt{(L+\lambda)P_{i\|k}}$ $i = 1,2,\dots,2L$ and $k = 1,2,\dots,N$ where, $\gamma = \sqrt{L+\lambda}$ and $\lambda = \alpha^2(L+K) - L$ So that it is obtained, $\gamma = \sqrt{\alpha^2(L+K)} = \alpha\sqrt{L+K}$
Prediction Step	Estimate $\chi^f_{i\|k} = f(\chi_{i\|k})$ $\hat{x}^-_{k+1} = \sum_{i=0}^{2L} W_i^m \chi^f_{i\|k}$ Error covariance $P^-_{k+1} = \sum_{i=0}^{2L} W_i^c (\chi^f_{i\|k} - \hat{x}^-_{k+1})(\chi^f_{i\|k} - \hat{x}^-_{k+1})^T + Q$
Correction (Update) Step	Measurement model, $Y^f_{i\|k} = H(\chi^f_{i\|k})$ $\hat{y}^-_{k+1} = \sum_{i=0}^{2L} W_i^m Y^f_{i\|k}$ $P_{\hat{y}_{k+1}\hat{y}_{k+1}} = \sum_{i=0}^{2L} W_i^c (Y^f_{i\|k} - \hat{y}^-_{k+1})(Y^f_{i\|k} - \hat{y}^-_{k+1})^T + R$ Measurement and state covariance, $P_{\hat{x}_{k+1}\hat{y}_{k+1}} = \sum_{i=0}^{2L} W_i^c (\chi^f_{i\|k} - \hat{x}^-_{k+1})(Y^f_{i\|k} - \hat{y}^-_{k+1})^T$
	Kalman gain,

E-ISSN: 2656-5846
P-ISSN: 2656-2286

System Model and Measurement Model
$K_{k+1} = P_{\hat{x}_{k+1}\hat{y}_{k+1}}\left(P_{\hat{y}_{k+1}\hat{y}_{k+1}}\right)^{-1}$
Estimate,
$\hat{x}_{k+1} = \hat{x}_{k+1}^{-} + K_{k+1}(y_k - H\hat{y}_{k+1}^{-})$
Error covariance,
$P_{k+1} = P_{k+1}^{-} - K_{k+1}P_{\hat{y}_{k+1}}\hat{y}_{k+1}K_{k+1}^{T}$

(Roger, 2020)

2.5. Mean Absolute Percentage Error (MAPE)

Mean Absolute Percentage Error (MAPE) is a standard metric used to evaluate the accuracy of forecasting and estimation methods, expressed as the average absolute percentage error. MAPE is employed to assess the accuracy of predicted results by comparing them with observed values. Each observation period is indexed by t, where $t = 1,2,\ldots,n$, and $n$denotes the total number of observations. The actual value at period $t$is represented by X_t, while the forecasted value for the same period is denoted as $\hat{X}_t$. A smaller MAPE value indicates a higher level of prediction accuracy. The formula used to compute the MAPE value is given as follows (Hyndman and Athanasopoulos, 2021),

$$MAPE = \frac{1}{n}\sum_{t=1}^{n}\left|\frac{X_t - \hat{X}_t}{X_t}\right| \times 100\%$$

Table 3 presents the interpretation of estimation results using the MAPE to determine the level of accuracy of the obtained results.

Table 3. MAPE Accuracy Level

MAPE	Estimation Accuracy Level
$< 10\%$	Very Accurate
$10\% \leq MAPE < 20\%$	Good
$20\% \leq MAPE < 50\%$	Fair
$\geq 50\%$	Not Accurate

3. Results and Discussion

In this study, the SEIR–SI dengue fever transmission model is estimated using the EnkF method. The discretized SEIR–SI model employed in this research is formulated as a nonlinear system, as described below,

$$\begin{bmatrix} S_{h_{k+1}} \\ E_{h_{k+1}} \\ I_{h_{k+1}} \\ R_{h_{k+1}} \\ S_{v_{k+1}} \\ I_{v_{k+1}} \end{bmatrix} = \begin{bmatrix} \Delta t\left(\lambda_h - \frac{\beta_h}{N_h}S_{h_k}I_{v_k} - \mu_h S_{h_k} + \theta R_{h_k}\right) + S_{h_k} \\ \Delta t\left(\frac{\beta_h}{N_h}S_{h_k}I_{v_k} - \delta E_{h_k} - \mu_h E_{h_k}\right) + E_{h_k} \\ \Delta t\left(\delta E_{h_k} - \gamma I_{h_k} - \mu_h I_{h_k}\right) + I_{h_k} \\ \Delta t\left(\gamma I_{h_k} - \mu_h R_{h_k} - \theta R_{h_k}\right) + R_{h_k} \\ \Delta t\left(\lambda_v - \frac{\beta_v}{N_h}S_{v_k}I_{h_k} - \mu_v S_{v_k}\right) + S_{v_k} \\ \Delta t\left(\frac{\beta_v}{N_h}S_{v_k}I_{h_k} - \mu_v I_{v_k}\right) + I_{v_k} \end{bmatrix} + \begin{bmatrix} w_{1_k} \\ w_{2_k} \\ w_{3_k} \\ w_{4_k} \\ w_{5_k} \\ w_{6_k} \end{bmatrix} \quad (9)$$

In equation (9), w_k denotes the process noise vector, which captures model uncertainties and stochastic variations in dengue fever transmission dynamics. It

E-ISSN: 2656-5846
P-ISSN: 2656-2286

is assumed to follow a zero-mean Gaussian distribution, $w_k \sim \mathcal{N}(0, Q)$, where Q is the process noise covariance matrix. The inclusion of process noise converts the deterministic SEIR–SI model into a stochastic state-space system, enabling EnKF and UKF to update state estimates by accounting for uncertainty in model evolution.

Tabel 4. Initial Values of Each Variable and Parameter

Variable	Initial Value	Parameter	Initial Value
S_h	43017127	λ_h	0.023757
E_h	6366	δ	0.125
I_h	3183	μ_h	0.000046
R_h	3151	θ_h	0.575
S_v	600000000	γ_h	0.328833
I_v	10000000	μ_v	0.0323
		β_h	0.75
		λ_v	0.5
		β_v	0.375

The data used in this study are secondary data consisting of the cumulative number of human populations infected with dengue fever transmission in West Java Province during the period 2010–2023, obtained from the Open Dengue website. The dataset comprises monthly data over 168 months, covering the period from January 2010 to December 2023. The simulation is conducted by assigning initial values to the system noise covariance matrix Q_k, namely $10^6, 10^4, 10^4, 10^3, 10^3$and 10^5, and the measurement noise covariance $R = 10^{-3}$. The initial values of the state variables are provided in Table 3. The measurement model used in this study is given as follows,

$$z_k = \begin{bmatrix} 0 & 1 & 0 & 0 & 0 & 0 \end{bmatrix} \begin{bmatrix} S_h \\ E_h \\ I_h \\ R_h \\ S_v \\ I_v \end{bmatrix} \tag{10}$$

In the observation model $z_k = Hx_k + v_k$, the term $v_k \sim \mathcal{N}(0, R)$represents measurement noise. In the implementation, this noise is not added as random values to the measurement data z_k at each step, instead, it is incorporated through the covariance matrix R during the Kalman update stage. The simulation results are as follows.

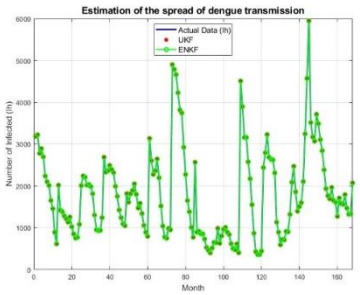

Figure 1. The Estimation Results for the Infected Human Population Capable of Transmitting the Virus

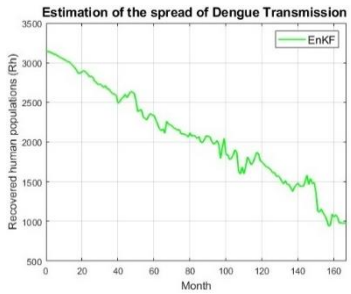

Figure 4. The Estimation Results for the Recovered Human Population

E-ISSN: 2656-5846
P-ISSN: 2656-2286

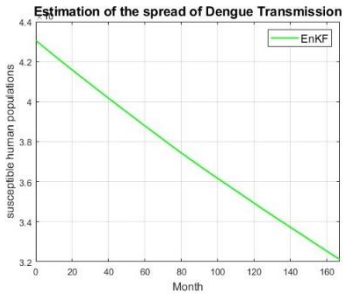

Figure 2. The Estimation Results for the Human Population Susceptible to Dengue Infection

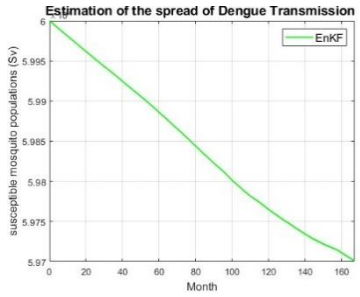

Figure 5. The Estimation Results for the *Aedes* Mosquito Population not yet Infected with the Dengue Virus

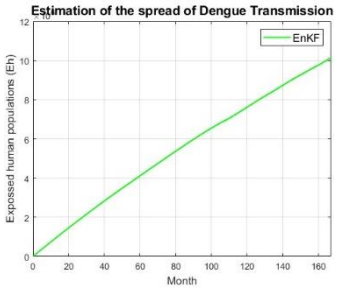

Figure 3. The Estimation Results for the Human Population Exposed to the Dengue Virus (Infected but not yet Infectious)

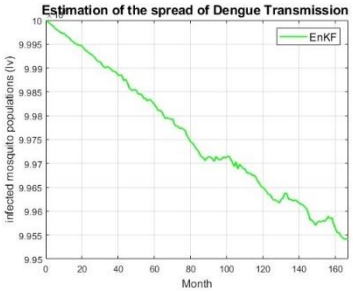

Figure 6. The Estimation Results for the Mosquito Population that has been Infected and Remains Capable of Transmitting the Dengue Virus throughout Its Lifetime

3.1. The Estimation Results for the Infected Human Population Capable of Transmitting the Virus

Figure 2 illustrates the estimation of the infected human population (I_h) in dengue fever transmission. The blue line represents the actual infected human population, obtained from the cumulative monthly dengue case data in West Java Province for the period 2010–2023. The green curve shows the estimated values generated using the EnKF which achieved a MAPE of 2.4%. Meanwhile, the red circles indicate the estimated values obtained using the Unscented Kalman Filter (UKF), with a MAPE of 7.8%.

These simulation results demonstrate that the EnKF provides a more suitable estimation method for the nonlinear dengue fever transmission model, as shown by its lower and more accurate MAPE value compared to the UKF. Based on the comparison presented in Figure 2, further estimation of other state variables using the EnKF can be performed. The estimated values for S_h, E_h, I_h, R_h, S_v, and I_v obtained using the EnKF are presented as follows.

3.2. The Estimation Results for the Human Population Susceptible to Dengue Infection

The simulation graph in Figure 3 presents the estimation of the susceptible human population (S_h) in the transmission of dengue fever transmission. The green curve represents the estimated values obtained using the EnKF method. The figure shows that the susceptible population exhibits a gradual decreasing trend on a monthly basis from early 2010 to the end of 2023. This decline is attributed to the

E-ISSN: 2656-5846
P-ISSN: 2656-2286

transition of individuals into the infected class through the infection rate, as well as natural mortality.

3.3. The Estimation Results for the Human Population Exposed to the Dengue Virus (Infected but not yet Infectious)

The simulation graph in Figure 4 presents the estimation of the exposed human population (E_h), representing individuals who have been infected with the dengue virus but are not yet capable of transmitting it, in the transmission of dengue fever transmission. The green curve represents the estimated values obtained using the EnKF method. The figure shows that the exposed population exhibits a gradual increasing trend on a monthly basis from early 2010 to the end of 2023. This increase occurs because the number of exposed individuals continues to rise over the study period, primarily due to the transition of individuals from the susceptible class to the exposed class.

3.4. The Estimation Results for the Recovered Human Population

The simulation graph in Figure 5 presents the estimation of the recovered human population (R_h). The green curve represents the estimated values obtained using the EnKF method. The figure shows that the recovered population exhibits fluctuations over certain periods; however, overall, it demonstrates a decreasing monthly trend from early 2010 to the end of 2023. This decline is attributed to a significant increase in new infections, which leads to a reduction in the number of recovered individuals over time.

3.5. The Estimation Results for the Aedes Mosquito Population not yet Infected with the Dengue Virus

The simulation graph in Figure 6 presents the estimation of the susceptible *Aedes* mosquito population (S_v) in the transmission of dengue fever transmission. The green curve represents the estimated values obtained using the EnKF method. The figure shows that the susceptible mosquito population exhibits a decreasing trend from 2010 to 2023. This decline is attributed to the transition of mosquitoes from the susceptible class to the infected class as a result of dengue virus transmission, leading to a reduction in the number of susceptible mosquitoes over time.

3.6. The Estimation Results for the Mosquito Population that has been Infected and Remains Capable of Transmitting the Dengue Virus throughout Its Lifetime

The simulation graph in Figure 7 presents the estimation of the dengue virus–infected mosquito population (I_v) in the transmission of dengue fever transmission. The green curve represents the estimated values obtained using the EnKF method. The figure shows that the infected mosquito population exhibits a decreasing trend from 2010 to 2023. This decline is primarily attributed to natural mosquito mortality, which reduces the number of infected mosquitoes over time.

4. Conclusions

This study implemented the Ensemble Kalman Filter (EnKF) and the UKF within a nonlinear SEIR–SI model to estimate the state variables of dengue fever transmission using cumulative monthly case data from West Java Province during 2010–2023. The integration of the dynamic model with a linear measurement model enabled the estimation of both the infected human population (Ih) and other

E-ISSN: 2656-5846
P-ISSN: 2656-2286

unobserved compartments. Simulation results show that EnKF achieved a MAPE of 2.4%, while UKF yielded 7.8%. Both methods fall within the high-accuracy category (MAPE < 10%); however, EnKF produced lower estimation error and demonstrated superior performance in reconstructing cumulative infection dynamics. This study is limited by the exclusion of environmental factors, population mobility, and spatial heterogeneity from the model structure. Nevertheless, the findings may support prediction-based dengue control policies by providing more measurable information on case dynamics. Future research may extend the model by incorporating external variables, such as climatological factors and population mobility, to represent dengue fever transmission dynamics more comprehensively.

Author Contributions

The first author was responsible for collecting, processing, and analyzing the data, as well as writing the scientific article. The second author contributed by offering feedback and suggestions to improve the study, its analysis, and the overall manuscript.

Acknowledgment

With gratitude, the author would like to express his gratitude to God Almighty for the abundance of His grace and gifts, so that the author can complete the writing of the article entitled "Estimation of Dengue Fever Transmission Model in West Java Using the Ensemble Kalman Filter Method". The author would also like to express his gratitude to the supervisor, the Head of the Master of Mathematics Study Program and his beloved family for all forms of support and direction that have been given during the process of compiling this article.

Declaration of Competing Interest

There are no indications of potential conflicts of interest disclosed by the authors.

References

Awaludin, Aziz, Harun Joko Prayitno, and Muhammad Izzul Haq. 2023. "Using Digital Media During the COVID-19 Pandemic Era:Good Online Program in Higher Education." *Indonesian Journal on Learning and Advanced Education* 5(2020): 1–12.

Bolan, Shiv et al. 2024. "Science of the Total Environment Impacts of Climate Change on the Fate of Contaminants through Extreme Weather Events." 909(August 2023).

Brajard, Julien, Alberto Carrassi, Marc Bocquet, and Laurent Bertino. 2021. "Combining Data Assimilation and Machine Learning to Infer Unresolved Scale Parametrization Subject Areas :" *Philosophical Transactions* 10(1098).

Carrassi, Alberto, and Marc Bocquet. 2018. "Data Assimilation in the Geosciences An Overview on Methods , Issues and Perspectives." *Wire climate change* 9(5).

Cohnstaedt, L E E W, and Caterina M Scoglio. 2021. "SEIR-SEI-EnKF : A New Model for Estimating and Forecasting Dengue Outbreak Dynamics." *IEEE Access* 9: 156758–67.

Hyndman, R. J., and G. Athanasopoulos. 2021. *Forecasting: Principles and Practice*. 3rd ed. OTexts. https://otexts.com/fpp3/.

Jiang, Shida, Junzhe Shi, and Scott Moura. 2025. "A New Framework for Nonlinear

E-ISSN: 2656-5846
P-ISSN: 2656-2286

Kalman Filters." (November).
Kementerian Kesehatan Republik Indonesia. 2024. "Situasi DBD Indonesia." (Informasi kasus DBD). https://www.kemkes.go.id/%0A (January 16, 2026).
Kularatne, S A M et al. 2025. "Clinical and Laboratory Predictors of Dengue Hemorrhagic Fever in a Resource-Limited Setting : A Prospective Observational Study From Sri Lanka." 17(11).
Li, Heng et al. 2025. "Improved Unscented Transformation Method and Its Application in Ship Uncertainty-Based Optimization." *Ocean Engineering* 339(P2): 122199. https://doi.org/10.1016/j.oceaneng.2025.122199.
Listosari, L. A. B. 2018. "Estimasi Gerak Proyektil Di Bawah Pengaruh Faktor Lingkungan Tropis Menggunakan Metode Unscented Kalman Filter." Institut Teknologi Sepuluh Nopember.
Liu, Zhuanzhuan et al. 2023. "The Effect of Temperature on Dengue Virus Transmission by Aedes Mosquitoes." *Frontiers in Cellular and Infection Microbiology* 13(September): 1–10.
Messina, Jane P et al. 2020. "The Current and Future Global Distribution and Population at Risk of Dengue." *Nature Microbiology* 4(September 2019). http://dx.doi.org/10.1038/s41564-019-0476-8.
Munch, Stephan B, Tanya L Rogers, and George Sugihara. 2022. "Recent Developments in Empirical Dynamic Modelling." *Ecology and Evolution* 2022(August): 732–45.
Namirimu, Teddy, and Sunjoo Kim. 2024. "Dengue Fever : Epidemiology , Clinical Manifestations , Diagnosis , and Therapeutic Strategies." 27(2): 131–41.
Narinder, Singh, Ajeet Pal Ajeet, and Amar Pal Amar Pal. 2022. "Dengue Virus : A Review." *Indian Journal of Pharmacy and Pharmacology* 8(4): 243–47.
Nasirian, Hassan. 2024. "The Introduction and Establishment of Dengue Disease in A New Area: A Mini Review." *Caspian Journal of Health Researc* 9(1): 51–56.
Papa, Michelle Premazzi et al. 2024. "Dengue NS1 Antibodies Are Associated With Clearance of Viral Nonstructural Protein-1." *The Journal of Infectious Diseases* 230(6): 1226–34. https://doi.org/10.1093/infdis/jiae299.
Papageorgiou, Vasileios E, and George Tsaklidis. 2022. "A Hybrid SEIHCRDV-UKF Model for COVID-19 Prediction . Application on Real-Time Data." *Research Square* 2.
Roger R, Labbe Jr. 2020. "Kalman and Bayesian Filters in Python."
Safitria, Rina, Didik Khusnul Arif, and Fatmawati. 2023. "Estimasi Nilai Model Penyebaran Penyakit Malaria Dengan Menggunakan Metode Ensemble Kalman Filter."
Singh, Himali, Kumar Vijay Mishra, and Arpan Chattopadhyay. 2024. "Inverse Unscented Kalman Filter." *IEEE Transactions on Signal Processing* 72: 2692–2709.
Tong, Juxiu, Yang Gu, and Kuan Cheng. 2024. "Using an Ensemble Kalman Filter Method for a Soil Nitrogen Transport Model in the Real Rice Field." *Journal of Hydrology* 645(PA): 132224. https://doi.org/10.1016/j.jhydrol.2024.132224.
Villela, Daniel A M. 2020. "Discrete Time Forecasting of Epidemics." *Infectious Disease Modelling* 5: 189–96. https://doi.org/10.1016/j.idm.2020.01.002.
Wijayanti, Juni, and Muhammad Fakhruddin. 2023. "Modeling and Descriptive Analysis of Dengue Cases in Palu City , Indonesia." *Physica A* 625: 129019. https://doi.org/10.1016/j.physa.2023.129019.
World Health Organization. 2024. "Dengue and Severe Dengue."

E-ISSN: *2656-5846*
P-ISSN: *2656-2286*

https://www.who.int/news-room/fact-sheets/detail/dengue-and-severe-dengue%0A (January 15, 2026).

Zeng, Qinghui et al. 2023. "Dengue Transmission Dynamics Prediction by Combining Metapopulation Networks and Kalman Filter Algorithm." *PLOS Neglected Tropical Diseases* 17(6): 1–20. http://dx.doi.org/10.1371/journal.pntd.0011418.

Zhang, Wei-xian et al. 2025. "Assessing the Global Dengue Burden : Incidence , Mortality , and Disability Trends over Three Decades." : 1–18. https://doi.org/10.1371/journal.pntd.0012932.